

HADRONS IN COVARIANT CONFINED QUARK MODEL* **

ANDREJ LIPTAJ , STANISLAV DUBNIČKA 

Institute of Physics, Slovak Academy of Sciences, Bratislava, Slovakia

ANNA Z. DUBNIČKOVÁ 

Faculty of Mathematics, Physics and Informatics, Comenius University
Bratislava, Slovakia

MIKHAIL A. IVANOV 

Independent Researcher

*Received 26 March 2025, accepted 11 September 2025,
published online 19 December 2025*

The Covariant Confined Quark Model is a reputed theoretical model acknowledged by important experimental groups. We provide a short overview of the model including several selected results.

DOI:10.5506/APhysPolBSupp.18.6-A22

1. Introduction

A decade or two ago, various heavy-quark factories having came into operation stimulating significant activity in fields of heavy-meson decays, multiquark states physics, and precision measurements (decay widths, branching fractions, electro-weak parameters). Despite important progress in theoretical approaches with small model dependence (notably the lattice QCD), the persisting difficulties related to hadronic corrections make quark models still one of the most appealing options. The Covariant Confined Quark Model (CCQM) [1] is an effective field theory approach suited for a unified description of different multiquark states based on a non-local hadron–quark interaction Lagrangian with quark confinement included.

* Presented at the V4-HEP 1 — Theory and Experiment in High Energy Physics Workshop, Bratislava, Slovakia, 26–28 July, 2023.

** Authors acknowledge the support from VEGA grant No. 2/0084/25.

2. Covariant Confined Quark Model

The quark current in the quark–hadron interaction Lagrangian given by $\mathcal{L}_{\text{int}}^{\text{CCQM}} = g_H H(x) J_H(x)$ takes a different form for mesons, baryons, and tetraquarks and, respectively, can be written as

$$J_M(x) = \int dx_1 \int dx_2 F_M(x, x_1, x_2) \bar{q}_{f_1}^a(x_1) \Gamma_M q_{f_2}^a(x_2), \quad (1)$$

$$\begin{aligned} J_B(x) = & \int dx_1 \int dx_2 \int dx_3 F_B(x, x_1, x_2, x_3) \\ & \times \Gamma_1 q_{f_1}^{a_1}(x_1) \left(q_{f_2}^{a_2}(x_2) C \Gamma_2 q_{f_3}^{a_3}(x_3) \right) \varepsilon^{a_1 a_2 a_3}, \end{aligned} \quad (2)$$

$$\begin{aligned} J_T(x) = & \int dx_1 \cdots \int dx_4 F_T(x, x_1, \dots, x_4) \left(q_{f_1}^{a_1}(x_1) C \Gamma_1 q_{f_2}^{a_2}(x_2) \right) \\ & \times \left(\bar{q}_{f_3}^{a_3}(x_3) \Gamma_2 C \bar{q}_{f_4}^{a_4}(x_4) \right) \varepsilon^{a_1 a_2 c} \varepsilon^{a_3 a_4 c}, \end{aligned} \quad (3)$$

where q are the quark fields, a_i and f_i the color and flavor indices, Γ_n an appropriate string of Dirac matrices, C the charge conjugation matrix, and F_H the vertex function. The latter takes the form

$$F_H(x, x_1, \dots, x_n) = \delta \left(x - \sum_{i=1}^n w_i x_i \right) \Phi_H \left(\sum_{i < j} (x_i - x_j)^2 \right), \quad (4)$$

$$w_i = \frac{m_i}{\sum_{j=1}^n m_j}, \quad \bar{\Phi}_H(-k^2) = \exp \left(\frac{k^2}{\Lambda_H^2} \right). \quad (5)$$

Here, m_i are the constituent quark masses (model parameters), Λ_H is a hadron-related model parameter, and $\bar{\Phi}_H$ is the momentum representation of the vertex function. This construction guarantees covariance. The Lagrangian formulation also allows one to rely on the usual QFT diagram techniques for computations. The CCQM does not contain gluons, these are implicitly considered through the vertex function tuned using the free hadronic parameter. Let us only mention a few other important aspects of the model:

- Interaction with photons: the free parts of the Lagrangian are gauged with the minimal subtraction scheme. In the strong-interaction part, a gauge-field exponential is introduced, similarly to [2].
- Since both, quark and hadron fields are present, the double counting needs to be addressed. We use the so-called compositeness condition expressed through the derivative of the particle's mass operator Π'_H , which requires the renormalization constant to vanish: $Z_H^{1/2} =$

$1 - 3g_H^2 \Pi'_H(m_H^2)/(4\pi) = 0$. It is reached by tuning the coupling g_H and it removes quark degrees of freedom from the space of physical parameters.

- The quark confinement is introduced through an infrared cutoff in the integral over the space of Schwinger parameters which appear when quark propagators are expressed using the Schwinger parameterization. The method has similarities to the confined-propagator approach, *i.e.* the cutoff removes the singularities introduced by quark propagators. The whole expression then becomes an entire function with no poles, indicating an absence of asymptotic single-particle quark states, see Section 2.3 of [3].

We often apply the model to describe weak decays of various heavy multi-quark states. On the quark level, we use existing effective theory results: we consider all relevant four-fermion operators whose actions are weighted by scale-dependent Wilson coefficients and whose values we take from the literature. The model then predicts transition form factor and leptonic decay constants, and consequently, decay widths and branching fractions.

The model predictions can be illustrated using the $B \rightarrow D_{(s)}^{(*)} + \pi(\rho)$ decays [4]. Hereunder (Figs. 1 and 2), we respectively present the spin structure table, relevant diagram topologies, predicted form factors, and results. An overall overshooting in data is seen, also observed by several other authors [5–7]. Some consider this observation as a sign of New Physics and label it a “novel puzzle”.

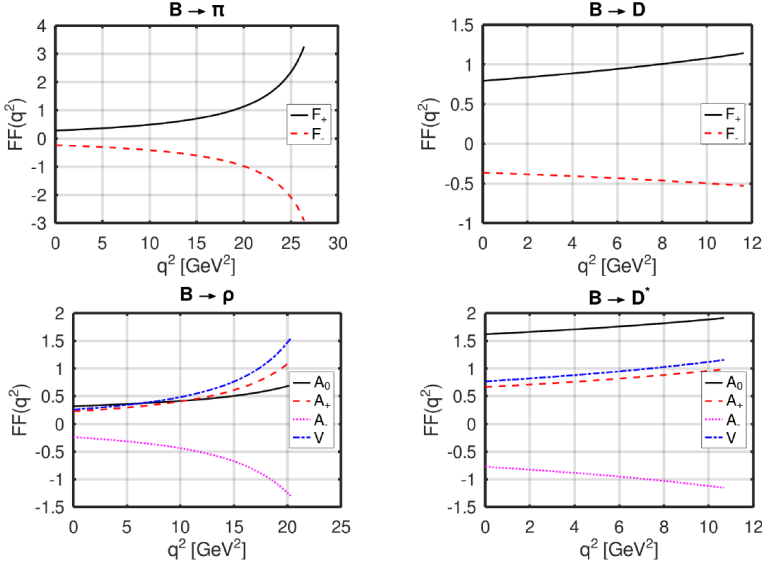
Spin structure	Diagram type		
	D_1	D_2	D_3
(A)	$B^0 \rightarrow D^- + \pi^+$ $B^0 \rightarrow \pi^- + D^+$ $B^0 \rightarrow \pi^- + D_s^+$ $B^+ \rightarrow \pi^0 + D_s^+$	$B^0 \rightarrow \pi^0 + \bar{D}^0$ $B^+ \rightarrow \bar{D}^0 + \pi^+$	
$PS \rightarrow PS + PS$			
(B)	$B^0 \rightarrow D^- + \varrho^+$ $B^0 \rightarrow \pi^- + D_s^+$ $B^+ \rightarrow \pi^0 + D^+$ $B^+ \rightarrow \pi^0 + D_s^{*+}$	$B^0 \rightarrow \pi^0 + \bar{D}^{*0}$ $B^+ \rightarrow \bar{D}^0 + \varrho^+$	
$PS \rightarrow PS + V$			
(C)	$B^0 \rightarrow D^{*-} + \pi^+$ $B^0 \rightarrow \varrho^- + D_s^+$ $B^+ \rightarrow \varrho^0 + D_s^+$	$B^0 \rightarrow \varrho^0 + \bar{D}^0$ $B^+ \rightarrow \bar{D}^{*0} + \pi^+$	
$PS \rightarrow V + PS$			
(D)	$B^0 \rightarrow D^{*-} + \varrho^+$ $B^0 \rightarrow \varrho^- + D_s^+$ $B^+ \rightarrow \varrho^0 + D_s^{*+}$	$B^0 \rightarrow \varrho^0 + \bar{D}^{*0}$ $B^+ \rightarrow \bar{D}^{*0} + \varrho^+$	
$PS \rightarrow V + V$			

(D_1)

(D_2)

(D_3)

Fig. 1. Processes: table with spin structure and diagrams.



	Process	Diagram	$\mathcal{B}_{\text{CCQM}}/\mathcal{E}$	$\mathcal{B}_{\text{PDG}}/\mathcal{E}$	\mathcal{E}
1	$B^0 \rightarrow D^- + \pi^+$	D_1	5.34 ± 1.07	2.52 ± 0.13	10^{-3}
2	$B^0 \rightarrow \pi^- + D^+$	D_1	11.19 ± 2.24	7.4 ± 1.3	10^{-7}
3	$B^0 \rightarrow \pi^- + D_s^+$	D_1	3.48 ± 0.70	2.16 ± 0.26	10^{-5}
4	$B^+ \rightarrow \pi^0 + D_s^+$	D_1	1.88 ± 0.38	1.6 ± 0.5	10^{-5}
5	$B^0 \rightarrow D^- + \rho^+$	D_1	14.06 ± 2.81	7.6 ± 1.2	10^{-3}
6	$B^0 \rightarrow \pi^- + D_s^{*+}$	D_1	3.66 ± 0.73	2.1 ± 0.4	10^{-5}
7	$B^+ \rightarrow \pi^0 + D^{*+}$	D_1	0.804 ± 0.16	< 3.6	10^{-6}
8	$B^+ \rightarrow \pi^0 + D_s^{*+}$	D_1	0.197 ± 0.04	< 2.6	10^{-4}
9	$B^0 \rightarrow D^{*-} + \pi^+$	D_1	4.74 ± 0.95	2.74 ± 0.13	10^{-3}
10	$B^0 \rightarrow \rho^- + D_s^+$	D_1	2.76 ± 0.55	< 2.4	10^{-5}
11	$B^+ \rightarrow \rho^0 + D_s^+$	D_1	0.149 ± 0.03	< 3.0	10^{-4}
12	$B^0 \rightarrow D^{*-} + \rho^+$	D_1	14.58 ± 2.92	6.8 ± 0.9	10^{-3}
13	$B^0 \rightarrow \rho^- + D_s^{*+}$	D_1	5.09 ± 1.02	4.1 ± 1.3	10^{-5}
14	$B^+ \rightarrow \rho^0 + D_s^{*+}$	D_1	0.275 ± 0.06	< 4.0	10^{-4}
15	$B^0 \rightarrow \pi^0 + \bar{D}^0$	D_2	0.085 ± 0.02	2.63 ± 0.14	10^{-4}
16	$B^0 \rightarrow \pi^0 + \bar{D}^{*0}$	D_2	1.13 ± 0.23	2.2 ± 0.6	10^{-4}
17	$B^0 \rightarrow \rho^0 + \bar{D}^0$	D_2	0.675 ± 0.14	3.21 ± 0.21	10^{-4}
18	$B^0 \rightarrow \rho^0 + \bar{D}^{*0}$	D_2	1.50 ± 0.30	< 5.1	10^{-4}
19	$B^+ \rightarrow \bar{D}^0 + \pi^+$	D_3	3.89 ± 0.78	4.68 ± 0.13	10^{-3}
20	$B^+ \rightarrow \bar{D}^0 + \rho^+$	D_3	1.83 ± 0.37	1.34 ± 0.18	10^{-2}
21	$B^+ \rightarrow \bar{D}^{*0} + \pi^+$	D_3	7.60 ± 1.52	4.9 ± 0.17	10^{-3}
22	$B^+ \rightarrow \bar{D}^{*0} + \rho^+$	D_3	11.75 ± 2.35	9.8 ± 1.7	10^{-3}

Fig. 2. Form factors and result table.

REFERENCES

- [1] T. Branz *et al.*, *Phys. Rev. D* **81**, 034010 (2010).
- [2] J. Terning, *Phys. Rev. D* **44**, 887 (1991).
- [3] S. Dubnička, A.Z. Dubničková, M.A. Ivanov, A. Liptaj, *Symmetry* **12**, 884 (2020).
- [4] S. Dubnička, A.Z. Dubničková, M.A. Ivanov, A. Liptaj, *Phys. Rev. D* **106**, 033006 (2022).
- [5] M. Bordone *et al.*, *Eur. Phys. J. C* **80**, 951 (2020).
- [6] S. Iguro, T. Kitahara, *Phys. Rev. D* **102**, 071701 (2020).
- [7] F.-M. Cai, W.-J. Deng, X.-Q. Li, Y.-D. Yang, *J. High Energy Phys.* **2021**, 235 (2021).